Fungal Genetics and Biology 86 (2016) 47–57

Contents lists available at ScienceDirect

Fungal Genetics and Biology

journal homepage: www.elsevier.com/locate/yfgbi

Highly efficient CRISPR mutagenesis by microhomology-mediated end joining in *Aspergillus fumigatus*

Chi Zhang, Xiuhua Meng, Xiaolei Wei, Ling Lu *

Jiangsu Key Laboratory for Microbes and Functional Genomics, Jiangsu Engineering and Technology Research Center for Microbiology, College of Life Sciences, Nanjing Normal University, Nanjing 210023, China

ARTICLE INFO

Article history:
Received 10 October 2015
Revised 30 November 2015
Accepted 9 December 2015
Available online 14 December 2015

Keywords:
CRISPR mutagenesis
Microhomology
In situ tag-insertion
Multi-locus genomic mutagenesis

ABSTRACT

Filamentous fungi have a dominant nonhomologous-end joining (NHEJ) DNA repair pathway, which results in the majority of transformed progenies having random heterologous insertion mutagenesis. Thus, lack of a versatile genome-editing tool prevents us from carrying out precise genome editing to explore the mechanism of pathogenesis. Moreover, clinical isolates that have a wild-type *ku80* background without any selection nutrition marker especially suffer from low homologous integration efficiency. In this study, we have established a highly efficient CRISPR mutagenesis system to carry out precise and efficient in-frame integration with or without marker insertion with approximately 95–100% accuracy via very short (approximately 35-bp) homology arms in a process referred to as microhomology-mediated end joining (MMEJ). Based on this system, we have successfully achieved an efficient and precise integration of an exogenous GFP tag at the predicted site without marker insertion and edited a conidial melanin gene *pksP* and a catalytic subunit of calcineurin gene *cnaA* at multiple predicted sites with or without selection marker insertion. Moreover, we found that MMEJ-mediated CRISPR-Cas9 mutagenesis is independent of the *ku80* pathway, indicating that this system can function as a powerful and versatile genome-editing tool in clinical *Aspergillus* isolates.

1. Introduction

Aspergillus fumigatus (*A. fumigatus*), the most common airborne fungal pathogenic species that exists ubiquitously in nature, is an increasingly fatal threat to immunocompromised patients worldwide (Wei et al., 2015). Global estimates suggest that the fungal pathogen genus *Aspergillus* is responsible for over 200,000 cases of invasive aspergillosis (IA) annually. Over 1.2 million patients are stricken with chronic pulmonary aspergillosis (CPA), and 4.8 million suffer from allergic bronchopulmonary aspergillosis (ABPA), with most infections being caused by *A. fumigatus* (Denning et al., 2011, 2013). Understanding the pathogenesis of *A. fumigatus in vitro* and *in vivo* has become a high priority in the past decades. Although sequencing information and the structural gene annotations of the *A. fumigatus* genome could be obtained from online genomics resources such as the *Aspergillus* Genome Database (AspGD), a large portion of genes that are likely involved in pathogen virulence and pathogenesis remain poorly understood. Moreover, the presence of numerous antifungal-drug-resistant *A. fumigatus* isolates has been increasing in clinics. This observation underscores the basic inadequacy of drug targeting and emphasizes the urgent need for new antifungal targets (Denning and Bromley, 2015). However, because eukaryotic pathogens and their hosts have close evolutionary relationships, specific drugs against fungal infections with few side effects remain limited (Hill et al., 2013). It is urgently necessary to develop versatile methods to search the specific peptide regions in the target protein so that blocking this region can kill or inhibit pathogen viability while causing fewer side effects to the host. Although classical gene deletion approaches by homologous integration using flanking regions longer than 1000-bp have been used to verify that the function of a gene is required for survival of the fungal pathogen (da Silva Ferreira et al., 2006), they are technically complicated and time-intensive in inducing homology-directed repair (HDR) in wild-type strains, especially in clinical isolates of *A. fumigatus.* In addition, in contrast to the model species *Aspergillus nidulans* (*A. nidulans*), where sexual reproduction is carried out efficiently (Dyer and O'Gorman, 2012), a reliable strategy of sexual reproduction in most *A. fumigatus* species has not been established. However, it has been reported that some special supermater pairs are able to complete sexual reproduction after a 4–8-week incubation in some required

* Corresponding author at: College of Life Sciences, Nanjing Normal University, No. 1 Wen Yuan Rd., Qi Xia Qu, Nanjing, China.
E-mail address: linglu@njnu.edu.cn (L. Lu).

http://dx.doi.org/10.1016/j.fgb.2015.12.007
1087-1845/

environments (O'Gorman et al., 2009; Sugui et al., 2011). It is thus very difficult to perform mutagenesis of multiple genes by sexual crossing in *A. fumigatus*, especially in clinical isolates without any nutritional selection marker. Even though there is a middle ground approach whereby the nutritional marker *pyrG*/*pyr4* (encoding orotidine-5′-phosphate decarboxylase) is recycled under the pressure of 5-FOA (Hu et al., 2007; Nielsen et al., 2006), it is time-consuming and inefficient. Moreover, it is impossible to site-specifically mutate genes by homologous integration at their original loci without marker insertion in order to analyze the function of the key residues because most filamentous fungi predominantly employ nonhomologous-end joining (NHEJ) (Fuller et al., 2015; Krappmann et al., 2006a). Thus, the lack of powerful and versatile genome-editing tools impedes the exploration of *A. fumigatus* pathogenesis for the purpose of developing better infection prevention and control measures.

The CRISPR (clustered regularly interspaced short palindromic repeats)-Cas9 system has emerged as a powerful tool for genome-editing across species (Doudna and Charpentier, 2014). This bi-component system consists of a Cas9 endonuclease and a single guide RNA (sgRNA) that recruits Cas9 to a site-specific target in the genome (Jinek et al., 2012). The sgRNA consisted of a 20-nt guide sequence (gRNA/Protospacer) hybridized to the target region followed by PAM (Protospacer Adjacent Motif) and a downstream chimeric scaffold sequence (gRNA scaffold) (Ran et al., 2013). The ribonucleoprotein complex composed of Cas9 and sgRNA could generate a double-stranded break (DSB) in the target region (Shalem et al., 2015). The nick generated by the ribonucleoprotein complex would be sealed by the endogenous repair mechanisms NHEJ and homology-directed repair (HDR) (Doudna and Charpentier, 2014; Ran et al., 2013; Shalem et al., 2015). Previous studies have verified that the CRISPR-Cas9 system is capable of inducing and enhancing mutagenesis efficiency through both the NHEJ and HDR pathways in many eukaryotic systems (Doudna and Charpentier, 2014). Moreover, the CRISPR system has been used to carry out loss-of-function studies for functional genes by inducing the endogenous NHEJ or HDR repair pathway in yeasts and filamentous fungi (DiCarlo et al., 2013; Jacobs et al., 2014; Liu et al., 2015b; Nodvig et al., 2015; Ryan et al., 2014). Remarkably, it recently has been reported that the CRISPR/Cas9 system can indeed be used for the efficient (25–53%) targeting of *A. fumigatus* through a mechanism independent of the homologous repair machinery (Fuller et al., 2015).

In this study, we have established a highly efficient CRISPR mutagenesis system with which we can efficiently target the genome and introduce changes via microhomology-mediated end joining (MMEJ) with only very short (approximately 35-bp) homology arms. Through this approach, we can carry out precise and efficient in-frame integration of an exogenous GFP tag at the predicted site without marker insertion (approximately 95–100% accuracy rate) and efficient mutagenesis of multiple endogenous genes. Moreover, we found that this MMEJ-mediated, highly efficient CRISPR mutagenesis occurs via a *ku80*-independent pathway, indicating that this system may serve as a powerful and versatile genome-editing tool in clinical *Aspergillus* isolates.

2. Materials and methods

2.1. Strains, media, and culture conditions

A list of all *A. fumigatus* strains used in this study is given in supplementary data (Table S1). Strains were routinely grown on the following media (Hu et al., 2007; Jiang et al., 2014). MM (minimal media) contained 1% glucose, 2% agar, 1 mL/L trace elements and 50 mL/L 20 × salt solution as described previously; YAG media contained 0.5% yeast extract, 2% agar, 2% glucose, and 1 mL/L trace elements; YUU media contained YAG, 5 mM uridine and 10 mM uracil. For the induction of Cas9 expression under the conditional promoter P_{niiA}, we employed a modified MM (MM-N) plus 10 mM magnesium nitrate. The MM-N contains 1% glucose, 2% agar, 50 mL/L 20 × salt solution without $NaNO_3$, and 1 mL/L trace minerals without $(NH_4)_6Mo_7O_{24}{\cdot}4H_2O$. In addition, the MM-N plus 10 mM ammonium tartrate was used to repress the expression of Cas9. The recipe for liquid media is identical to that for the relative solid media but without agar. The strains were cultured at 37 °C for 2–3 days.

2.2. Plasmids construction

Primers used for plasmid construction and for repair templates were listed in Table S2 and primers used for diagnostic PCR and sequencing were given in Table S3. The Cas9-expressing plasmid P_{gpdA}-Cas9-Pyr4 (FM-1) was generated as follows. Using pX330 as PCR template, a 4328-bp fragment containing *cas9* ORF, NLS (nuclear localization signal) and FLAG were generated by PCR with the primers Cas9-ClaI-F and Cas9-ClaI-R. Then, using the One Step Cloning Kit (Vazyme, C114-01) this 4328-bp fragment was cloned into the *ClaI* site of pBARGPE, which contains a *gpdA* promoter (P_{gpdA}) and a trpC terminator (T_{trpC}) flanking the *ClaI* site. The P_{gpdA}-Cas9-T_{trpC} cassette amplified using primers Gpd-F and TrpC-R was cloned into the pEASY-Blunt Zero vector (TransGen Biotech) to generate the plasmid pP_{gpdA}-Cas9. As a selection marker, the 2.1-kb *pyr4* gene (a homolog of *pyrG*) from *Neurospora crassa* was amplified by PCR using the primers Pyr4-SpeI-F and Pyr4-SpeI-R. The *pyr4* PCR product was subcloned into the *SpeI* site of P_{gpdA}-Cas9, forming the plasmid pP_{gpdA}-Cas9-Pyr4 (FM-1).

The Cas9-expressing plasmid pP_{niiA}-Cas9-Pyr4 (FM-2) was generated as follows: the *niiA* promoter (P_{niiA}) fragment was amplified from the genomic DNA (gDNA) of the strain Af293 by PCR with primers NiiA-F and NiiA-R. The Cas9-T_{trpC} cassette was amplified from plasmid FM-1 using primers NiiA-Cas9-F and TrpC-R. Then, the *niiA* promoter and Cas9-T_{trpC} fragments were fused together with NiiA-F and TrpC-R. The fusion fragment was cloned into the pEASY-Blunt Zero vector, creating pP_{niiA}-Cas9. As described above, p_{niiA}-Cas9-Pyr4 (FM-2) was constructed by cloning the *pyr4* marker into the *SpeI* site of pP_{niiA}-Cas9.

The *pksP*-sgRNA1-expressing plasmid $pP_{U6\text{-}1/2/3}$-*pksP*-sgRNA1 (FM-4-1/2/3) was generated as follows. The gRNA scaffold sequence containing double *BBsI* sites was amplified from pX330 using primers gRNA-scaffold-F and gRNA-R. The three predicted *A. fumigatus U6* promoters (400-bp) were amplified from the Af293.1 genome by PCR with primers U6-1/2/3-F and U6-1/2/3-R appended with a complementary joint to the 5′ of the gRNA scaffold sequence. Then, the three *U6* promoter fragments were respectively fused to the gRNA scaffold fragment by fusion PCR with U6-1/2/3-F and gRNA-R. The three fusion fragments were cloned into the pEASY-Blunt Zero vector, creating the corresponding plasmids FM-3-1/2/3. To create $pP_{U6\text{-}1/2/3}$-*pksP*-sgRNA1 (FM-4-1/2/3), the DNA sequence (double BBsI sequence) between the *U6* promoter and the gRNA scaffold sequence in the FM-3-1/2/3 was replaced by the 20-bp *pksP*-gRNA1 sequence, which was performed by Restriction-free cloning system (http://www.rf-cloning.com) with primers U6-1/2/3-pksP1-R and PksP1-sgRNA-F.

pAMAI-P_{gpdA}-Cas9 and pAMAI-$P_{U6\text{-}3}$-*pksP*-sgRNA1-P_{gpdA}-Cas9 were constructed as follows. The P_{gpdA}-Cas9-T_{trpC} cassette was amplified from FM-1 by PCR with primers Gpd-NotI-F and TrpC-NotI-R. The fragment was cloned into the NotI site of FM-4-3 using the One Step Cloning Kit, creating the plasmid $pP_{U6\text{-}3}$-*pksP*-sgRNA1-P_{gpdA}-Cas9 (FM-5). Then, the P_{gpdA}-Cas9-T_{trpC} cassette was amplified with primers Gpd-BamHI-F and TrpC-BamHI-R and the $P_{U6\text{-}3}$-*pksP*-sgRNA1-P_{gpdA}-Cas9-T_{trpC} cassette was amplified

from plasmid FM-5 with primers U6-3-BamHI-F and TrpC-BamHI-R. The two fragments digested by *BamHI* were ligated into the corresponding sites of prg3-AMAI-*NotI* (Aleksenko and Clutterbuck, 1997), which contains a selectable *pyr4* marker, yielding the plasmids pAMAI-P_{gpdA}-Cas9 (FM-6) and pAMAI-P_{U6-3}-*pksP*-sgRNA1-P_{gpdA}-Cas9 (FM-7).

2.3. DNA repair templates for genetic manipulation

The linear P_{U6-3}-*pksP*-sgRNA1 fragments were amplified from FM-4-3 by PCR with primers U6-3-F and gRNA-R. The selection marker *hph-f1* fragments (gene product confers resistance to hygromycin B) flanked by two 39-bp microhomology arms (MHAs) located proximally to the target sequence of *pksP*-sgRNA1 were amplified from pAN7-1 by PCR with primers 39-pksP1-HPH-F and 39-pksP1-HPH-R (Gravelat et al., 2012). The *hph* alone was amplified from pAN7-1 by PCR with primers HPH-F and HPH-R. The *hph-f2* fragments flanked by two 28-bp MHAs located proximally to the target sequence of *cnaA*-sgRNA1 were amplified by PCR with primers 28-cnaA1-HPH-F and 28-cnaA1-HPH-R. The GFP fragments flanked by two 39-bp MHAs located proximally to the target sequence of *cnaA*-sgRNA2 were amplified from pLB-01 by PCR with primers 39-cnaA2-GFP-F and 39-cnaA2-GFP-R. To generate a 476-bp repair template (pksP2-f1) that contains two premature stop codons as a substitute for the PAM of *pksP*-sgRNA2, the 5′ and 3′ flanking DNA fragments were amplified from the gDNA of Af293 using the primers PksP-sgRNA2-p1and PksP-sgRNA2-p2, and PksP-sgRNA2-p3 and PksP-sgRNA2-p4, respectively. Then, the two PCR products were fused together using the primers PksP-sgRNA2-p1 and PksP-sgRNA2-p4, creating the 476-bp DNA repair template.

2.4. In vitro synthesized sgRNA

dsDNA template for sgRNA *in vitro* transcription were generated using PCR to amplify the sgRNA scaffold sequence from plasmid FM-3-2 using primers gRNA-R and T7-gRNA-F, which contains an 18-nt T7 promoter sequence, a 20-nt gRNA sequence and an approximately 20-nt sequence complementary to the 5′ end of the gRNA scaffold. Following the manufacturer's instructions, the 100 ng template purified by Biospin Gel Extraction Kit (BioFlux, Cat#BSC02M1) was transcribed into RNA *in vitro* using the MEGAscript T7 Kit (Ambion, Life Technologies). Then, the RNA product was purified by phenol/chloroform extraction solution followed by isopropanol precipitation. The purified RNA was dissolved in nuclease-free water.

2.5. Transformation

Transformation of *A. fumigatus* was performed according to a previously described procedure (Jiang et al., 2014). For sgRNA transformation, more than 4 μg RNA (*In vitro* synthesized sgRNA) and 5 μg DNA repair template were co-transformed into isolated protoplast as protocol recommended and other transformation procedures were carried out as described in (Jiang et al., 2014). Transformants were selected in the medium without uridine and uracil or in the presence of hygromycin B (150 μg/mL).

2.6. Plate assays, purification of transformants

A 2-μL sterile aqueous suspension containing the moderate spores of transformants was spotted onto YAG medium. After culturing for 2 days at 37 °C, the colonies were observed and imaged unless stated otherwise. Before verification, all candidate transformants were streak purified on YAG medium.

2.7. Diagnostic PCR and sequencing

All isolates were verified by diagnostic PCR or sequencing analysis using mycelium as the source of DNA. Primers for indels analysis were designed to bind upstream and downstream of the expected cleavage sites. To validate *hph* gene insertion, the additional two PCR reactions were generally carried out using two pairs of primers in which one primer binds the upstream or downstream region of PAM and the other primer binds inside the selective marker.

2.8. Western blotting

To extract proteins from *A. fumigatus* mycelia, 10^8 conidia were inoculated in liquid YAG or modified MM plus 10 mM magnesium nitrate/ammonium tartrate and then shaken at 220 rpm on a rotary shaker at 37 °C for 24 h. The tissue collected by filtration was ground in liquid nitrogen with a mortar and pestle and suspended in ice-cold extraction buffer (50 mM HEPES pH 7.4, 137 mM KCl, 10% glycerol containing, 1 mM EDTA, 1 μg/mL pepstatin A, 1 μg/mL leupeptin, and 1 mM PMSF). Equal amounts of protein per lane (unless otherwise stated) were subjected to 10% SDS–PAGE and transferred to a PVDF membrane (Immobilon-P, Millipore) in 384 mM glycine, 50 mM Tris (pH 8.4), and 20% methanol at 250 mA for 1.5 h. The membrane was then blocked with PBS, 5% milk, and 0.3% Tween 20. Next, the membrane was sequentially probed with 1:3000 dilutions of anti-FLAG and goat anti-rabbit IgG-horseradish peroxidase diluted in PBS, 5% milk, and 0.3% Tween 20, and the blot was developed by chemiluminescence (ECL, Amersham).

2.9. Microscopy and image processing

For microscopic observation, the fresh conidia were inoculated onto sterile glass coverslips overlaid with 1 mL of YAG liquid media. Strains were cultivated on the coverslips at 37 °C for 12 h before observation under a microscope. The coverslips with hypha were gently washed with PBS three times. Differential interference contrast (DIC) and green fluorescent images of the cells were collected with a Zeiss Axio Imager A1 microscope (Zeiss, Jena, Germany). These images were then collected and analyzed with a Sensicam QE cooled digital camera system (Cooke Corporation, Germany) and the MetaMorph/MetaFluor combination software package (Universal Imaging, West Chester, PA), and the results were assembled in Adobe Photoshop 7.0 (Adobe, San Jose, CA).

3. Results

3.1. Expression of human-codon–usage-bias Cas9 (hCas9) in A. fumigatus

Generally, establishing an efficient CRISPR-Cas9 system in a new species requires optimizing the codons of *cas9* gene originally obtained from bacterial *Streptococcus pyogenes* (Jinek et al., 2012; Liu et al., 2015b). Because there is a commercially available plasmid (pX330) that includes a codon-optimized human *cas9* gene (*hcas9*) with FLAG tag and NLS sequence, we next checked whether it is suitable for *A. fumigatus* based on the information provided by the codon usage database (http://www.kazusa.or.jp/codon/). We found that *A. fumigatus* possesses a codon usage bias similar to *Homo sapiens*. We next constructed this *hcas9* gene under the control of a strong fungal constitutive promoter P_{gpdA} accompanied by T_{trpC} as a fungal transcription terminator (Fig. 1A). The plasmid containing the P_{gpdA}-Cas9-T_{trpC} cassette and a *pyr4* marker was transformed into the *A. fumigatus* strain Af293.1, which is derived

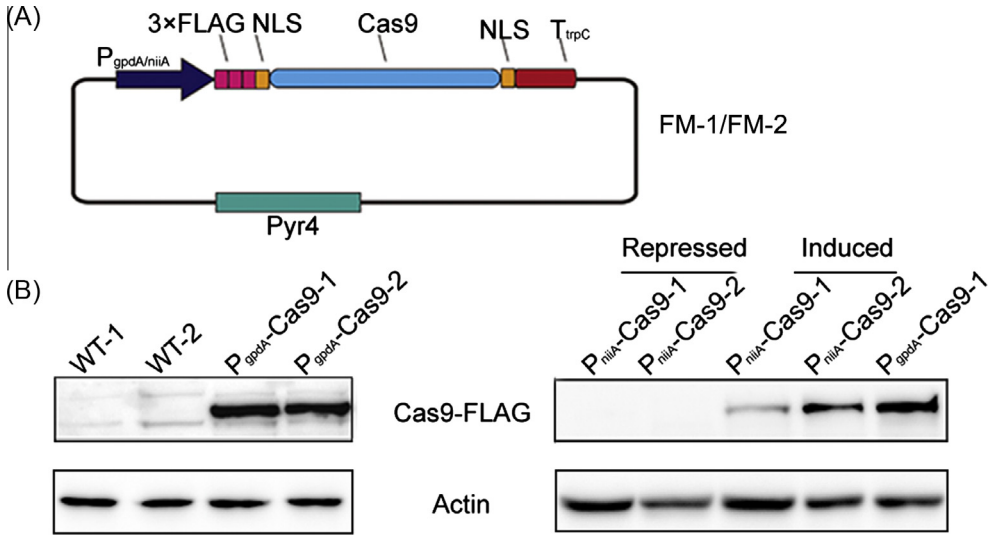

Fig. 1. Western blots showing the expression of Cas9-FLAG in *A. fumigatus*. (A) Schematic illustration of the plasmids expressing Cas9. FM-1 refers to the P_{gpdA}-Cas9-Pyr4 plasmid and the FM-2 refers to the P_{niiA}-Cas9-Pyr4 plasmid. (B) Left panel: Detection of Cas9-FLAG expression under the fungal constitutive promoter P_{gpdA} compared to that in the parental wild-type strain (WT) Af293. Right panel: Detection of Cas9-FLAG expression under the conditional promoter P_{niiA}. The inducing medium was composed of modified MM (MM-N) plus 10 mM magnesium nitrate, and the repressing medium was MM-N plus 10 mM ammonium tartrate. P_{gpdA}-Cas9-1/2 indicated strains ZC01-1/2, P_{niiA}-Cas9-1/2 indicated ZC02-1/2. Detailed strain genotypes can be found in Table S1. All lanes were loaded with same amount of proteins and the actin indicated a loading control.

from selection of *A. fumigatus* Af293 and is a uracil auxotroph strain (Xue et al., 2004). The expression of the Cas9 protein was detected after transformants were cultured in liquid YG medium for 24 h (Fig. 1B). Using an anti-FLAG antibody, our Western blots detected a specific band at approximately 164 kDa, the predicted size of the Cas9-FLAG fusion protein, indicating that *hcas9* can be expressed normally and specifically in *A. fumigatus*. Next, we tested whether *hcas9* could be conditionally expressed in *A. fumigatus*. Previous studies have demonstrated that P_{niiA} (the promoter of the *A. fumigatus* gene *niiA*) can be induced by nitrate and repressed by ammonium in media (Hu et al., 2007). We replaced the aforementioned P_{gpdA} with P_{niiA} and then tested the expression of *hcas9* under two different nitrogen culture conditions. As expected, the FLAG-fusion protein was detected at the predicted size, with a band at approximately 164 kDa in transformants grown in media where nitrate was the sole nitrogen source. We did not detect such a band under the repressed condition in which ammonium served as the nitrogen source (Fig. 1B), suggesting that replacement of the *gpdA* promoter with the *niiA* promoter enables a stringent conditional expression of *hcas9*. Taken together, our data demonstrated that *hcas9*, without any codon usage bias modification, could be expressed robustly and conditionally using a strong fungal constitutive *gpdA* promoter or a nitrogen-conditional *niiA* promoter.

3.2. A duet CRISPR-Cas9 system for A. fumigatus under the control of predicted RNA polymerase III-based U6 promoters

An efficient CRISPR system requires both the enzyme Cas9, which cleaves DNA, and an engineered sgRNA that is controlled by the appropriate promoter recognized by RNA polymerase III, such as the *RNU6-1* promoter in *Homo sapiens* and the *SNR52* promoter in *Candida albicans* and *Saccharomyces cerevisiae* (DiCarlo et al., 2013; Hsu et al., 2013; Vyas et al., 2015). Based on bioinformatics analysis, we found that there are 3 copies of predicted RNA polymerase III-based *U6* snRNA genes in *A. fumigatus*, referred to as *U6-1*, *U6-2*, and *U6-3*, in which all promoters share approximately 65% identity to the human *RNU6-1* sequence (Fig. 2A). Next, we try to express the sgRNA using three 400-bp DNA sequences predicted to be RNA polymerase III-based *U6* promoters (P_{U6-1}, P_{U6-2}, P_{U6-3}) in which the transcription start site of *U6* snRNA (non-coding RNA) is "G" in *A. fumigatus*. To further test the feasibility of the Cas9-sgRNA system described above, we chose *pksP* as a mutagenesis target gene because *ΔpksP* colonies confer a visible conidial pigmentless albino phenotype (Langfelder et al., 1998; Tsai et al., 1998). According to the designed approaches for the guide RNA presented by previous studies, a 20-nt target sequence in the front of PAM site was chosen to introduce a cleavage site by Cas9 nuclease (Doudna and Charpentier, 2014; Farboud and Meyer, 2015). The sgRNA sequence containing the 20-nt target of *pksP* was referred to as *pksP*-sgRNA1. Then, three constructs composed of a P_{U6-1}/P_{U6-2}/P_{U6-3}-*pksP*-sgRNA cassette were co-transformed with the Cas9 embedding plasmid pP_{gpdA}-Cas9-pyr4 (FM-1) into the recipient strain Af293.1 (Fig. 2B). We increased the ratio of the plasmid containing P_{U6}-*pksP*-sgRNA cassette to the FM-1 plasmid to make sure each *pyr4*-containing transformant having the multiple copies of sgRNA. As a result, a few predicted albino colonies or sectors were displayed on transformation plates, particularly on the plate transformed by the P_{U6-3}-*pksP*-sgRNA1 cassette, which conferred about a 43% mutation rate among all transformants (Fig. 2C). However, surprisingly, it seems as if all the albino transformants generated two types of albino progeny colonies grown on YAG medium (Fig. 2D). To further examine mutagenesis in details, we isolated 6 purified clones from the 4 independent albino transformants and performed diagnostic PCR to check indels of *pksP* mutagenesis. Surprisingly, we could not obtain any PCR products from the isolated albino colonies upon using primers that spanned adjacent predicted edited-site, suggesting that unpredicted indels may occur in the *pksP* locus with its adjacent genes (Figs. 2D and S1A). These data suggest that the duet CRISPR-Cas9 system for *A. fumigatus* under the control of predicted RNA polymerase III-based *U6* promoters could result in low accuracy genome editing.

3.3. A solo CRISPR-Cas9 system for A. fumigatus under the control of predicted RNA polymerase III-based promoters

Since the separate plasmids may cause the transformant to be embedded only either by the *cas9* gene or the sgRNA sequence resulted in "unpredicted indels" as well as the low mutagenesis

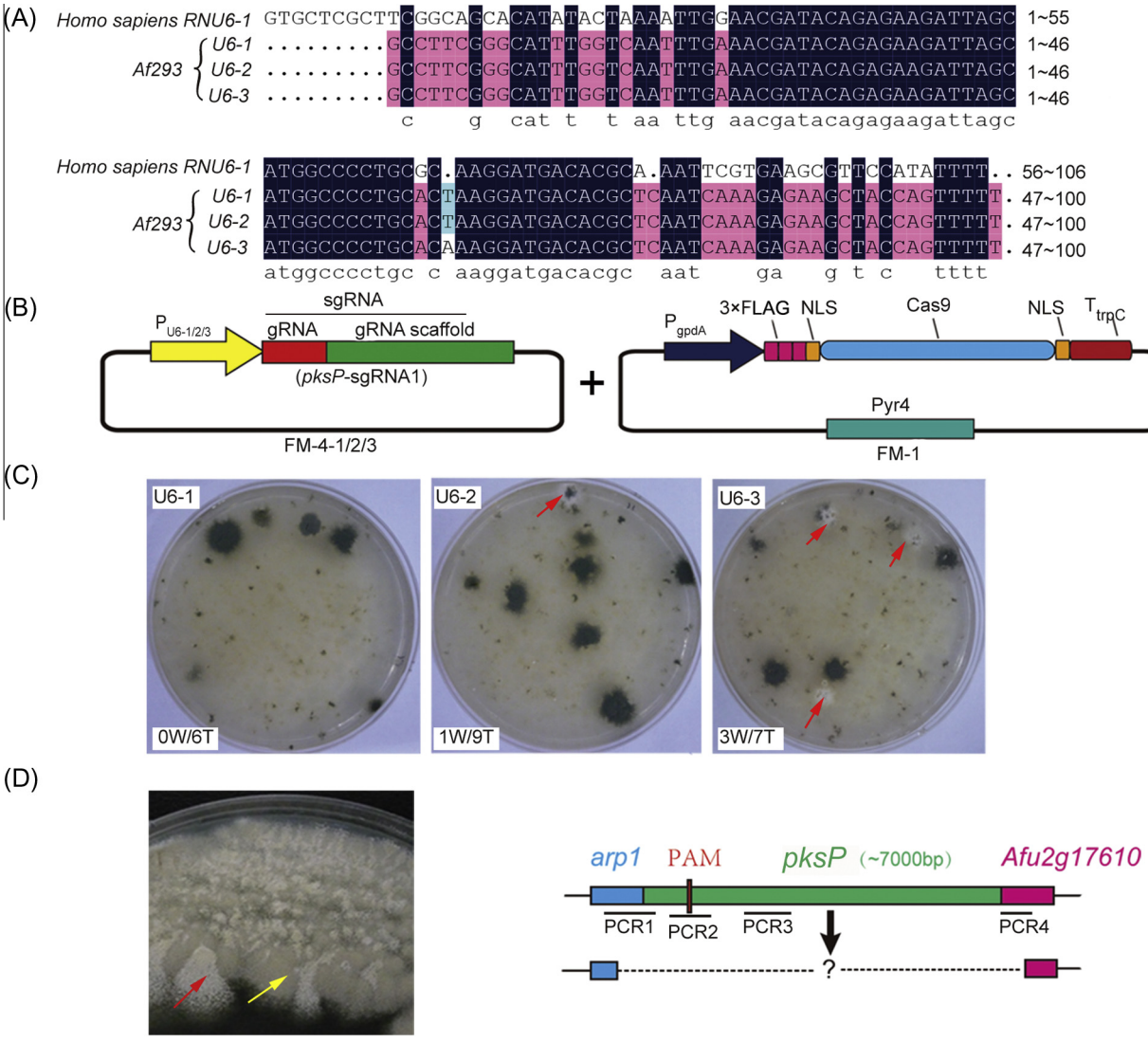

Fig. 2. A duet CRISPR-Cas9 system for *A. fumigatus* under the control of predicted RNA polymerase III-based U6 promoters. (A) Nucleotide blast between *Homo sapiens RNU6-1* and three *A. fumigatus U6* snRNA sequences. (B) Diagram of the duet CRISPR-Cas9 system, which consists of two plasmids, FM-4-1/2/3 (for expression of *pksP*-sgRNA1), FM-1 (for expression of Cas9). (C) The three transformation plates produced by co-transforming FM-4-1/2/3 and FM-1 into Af293.1. The 0W/6T indicated there are 0 albino colonies among all transformants on the transformation plate. (D) (Left) The albino colonies from the transformation plates were streak inoculated onto YAG medium for two days. The red and yellow arrows label two types of albino colonies. (Right) Schematic illustration of the diagnostic PCR against the isolated 6 albino colonies, which were derived from the 4 albino transformants, respectively. Detailed AGE (agarose gel electrophoresis) images can be found in the Supplementary data. (For interpretation of the references to color in this figure legend, the reader is referred to the web version of this article.)

efficiency. We next constructed a solo CRISPR-Cas9 system by inserting $P_{U6\text{-}3}$-*pksP*-sgRNA1 and P_{gpdA}-Cas9-T_{trpC} cassettes into the pAMA1 vector, which contains a *pyr4* marker (Fig. 3A) (Aleksenko and Clutterbuck, 1997). The *pksP* gRNA sequence and recipient strain were the same as described above for the duet system. We could not find any detectable albino colonies in any of the transformation plates; instead, all colonies retained green conidia. However, when the original transformants were streaked further, some of the albino colonies were clearly isolated in progenies of all independent transformants (Fig. 3B). To confirm the albino phenotype results from specific sgRNA-guided mutagenesis of *pksP*, PCR fragments (approximately 1-kb) covering the predicted Cas9 cleavage sites were generated from all six isolated albino colonies. The six PCR fragments were sequenced, and all of the cases displayed a 1-bp (A or T) insertion upstream of the PAM site (Fig. 3C). Therefore, compared to the duet CRISPR-Cas9 system, the solo CRISPR-Cas9 system is able to induce relatively accurate genome editing, albeit still with low efficiency.

3.4. Microhomology arms located proximally to the PAM site result in dramatic and highly efficient CRISPR mutagenesis

Based on our above data, we hypothesized that our solo and duet CRISPR-Cas9 systems for *A. fumigatus* might not be suitable for efficiently targeting the genome and introducing changes via NHEJ during the repair of double-strand DNA breaks (DSBs). Thus, we next attempted to test the functionality of homology-directed repair by CRISPR-Cas9 in *A. fumigatus*. To eliminate the influence of NHEJ repair and ensure an adequate expression of Cas9, the $A1160^{PgpdA\text{-}Cas9}$ (ZC03) that constitutively expresses Cas9 and lacks the NHEJ-required gene *ku80* was used as the recipient strain (da Silva Ferreira et al., 2006). To set up the homology arm, the relative 39-bp microhomology arms (MHAs) located proximally to the PAM site were added to both sides of the selection marker *hph*. After co-transformation with the linear $P_{U6\text{-}3}$-*pksP*-sgRNA1 fragments and the *hph* selection marker flanked by the above described MHAs under the hygromycin selection, we found that approximately

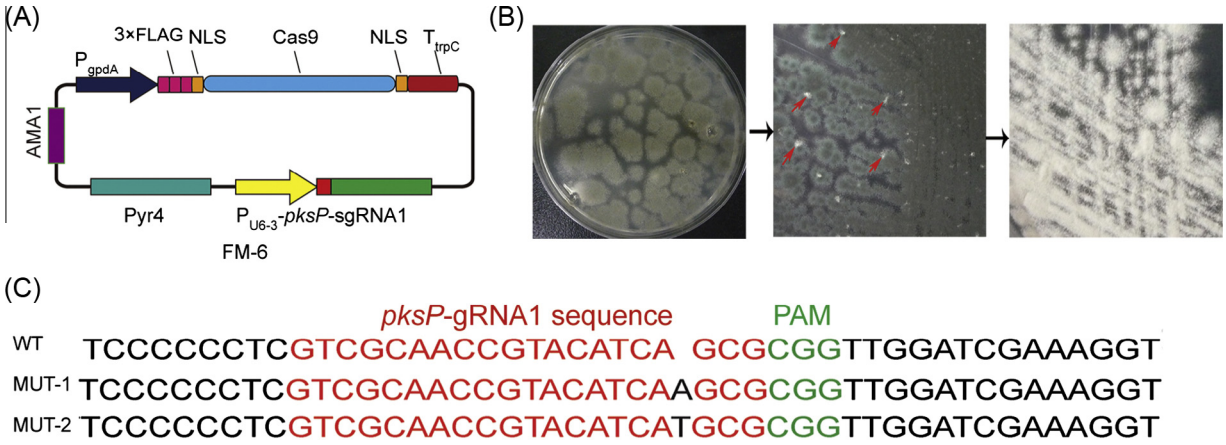

Fig. 3. The solo CRISPR-Cas9 system for *A. fumigatus* under the control of predicted RNA polymerase III-based U6 promoters. (A) The diagram of plasmid FM-6 for the solo CRISPR-Cas9 system. (B) The transformed albino colonies from solo CRISPR-Cas9 system showing further phenotype segregation in the isolated progenies on YAG medium. (C) A diagram showing the sequence of *pksP*-gRNA1 (red color) in mutants (MUT-1, MUT-2) and WT. (For interpretation of the references to color in this figure legend, the reader is referred to the web version of this article.)

67% of transformants on the transformation plate could be classified as albino colonies (Fig. 4A). In comparison, there were no detectable albino colonies present on the control transformation plate which had been transformed with the linear $P_{U6\text{-}3}$-*pksP*-sgRNA1 fragments with *hph* alone (Fig. 4B). Further diagnostic PCR demonstrated that all isolated albino transformants had the expected cleavage sites in the *pksP* locus with an insertion of the *hph* selectable marker (Fig. S1B). In contrast to standard homologous integration with homology arms at least 500-bp or 1000-bp in length (da Silva Ferreira et al., 2006), our data suggest that marker flanked by two very short homology arms is enough to repair the cleavage generated by the CRISPR-Cas9 system in *A. fumigatus*. These data suggest that microhomology-mediated end joining (MMEJ) is an efficient way to induce CRISPR mutagenesis in Cas9-expressing A1160 strain; we refer to it as the MMEJ- CRISPR system.

3.5. Highly efficient CRISPR mutagenesis induced by MMEJ is Ku-independent

In order to test whether the aforementioned MMEJ-CRISPR system could efficiently and precisely edit other genes, we next chose the functionally identified gene *cnaA* as a target. CnaA is a catalytic subunit of a eukaryotic Ca^{2+}- and calmodulin-dependent serine/threonine protein phosphatase-Calcineurin (Fox and Heitman, 2002; Liu et al., 2015a). Previous studies have verified that dysfunction of CnaA results in remarkable hyphal growth defects with a very small compacted colony phenotype (da Silva Ferreira

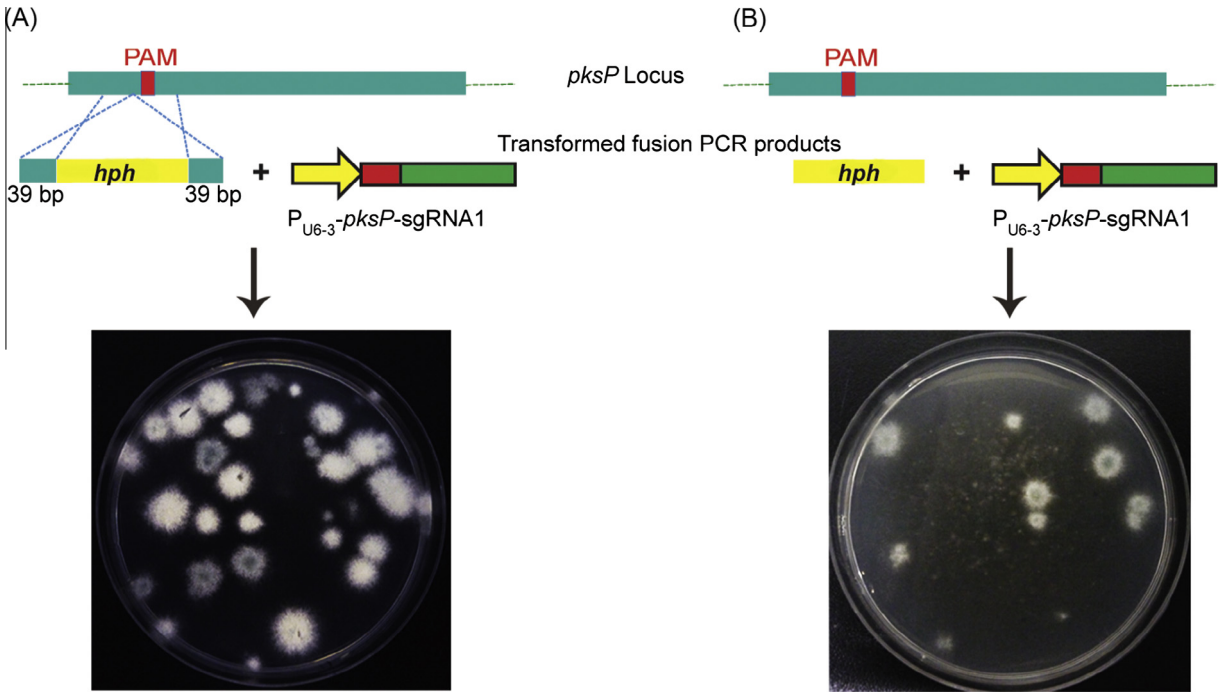

Fig. 4. A pair of microhomology arms located proximally to the PAM site dramatically results in highly efficient CRISPR mutagenesis. (A) (Up) Schematic illustration of the linear $P_{U6\text{-}3}$-*pksP*-sgRNA1 cassette and *hph* gene flanked with MHAs located proximally to the PAM site. (Bottom) The transformation plate derived by introducing the two aforementioned exogenous fragments into ZC03. (B) (Up) Schematic illustration of the construction for linear $P_{U6\text{-}3}$-*pksP*-sgRNA1 cassette and *hph* alone. (Bottom) The transformation plate for control.

et al., 2007; Steinbach et al., 2006). To improve the specificities of Cas9 nucleases, we designed a sgRNA containing an 18-nt truncated gRNA located within the first exon of *cnaA* (Fu et al., 2014), termed *cnaA*-sgRNA1, which was efficiently synthesized by *in vitro* transcription. After co-transformation with synthesized *cnaA*-sgRNA1 with *hph* fragments flanked by 28-bp MHAs located proximally to the expected cleavage site into ZC03 (Fig. 5A), we obtained numerous transformants on the transformation plates. To further dissect the phenotypes of the transformants, we randomly inoculated 39 colonies without purification onto YAG medium. Excitingly, all colonies had a phenotype similar to that of *ΔcnaA* (Fig. 5B). Further diagnostic PCR demonstrated that all of the six colonies tested had the expected cleavage site with an insertion of the *hph* selectable marker (Fig. S2A). As a control, the same amount of *cnaA*-sgRNA was co-transformed with the selection marker *hph* without MHAs into ZC03. Unexpectedly, there were no detectable hygromycin resistant transformants at all in three independent experiments on the control transformation plate. Next, we wondered whether the aforementioned MMEJ-CRISPR system could efficiently and precisely edit genes in a clinic-derived strain that includes the wild-type *ku80* gene. In order to eliminate the influence of *ku80* deletion, the Cas9 constitutively expressing strain ZC04, which retained a wild-type *ku80* gene derived from Af293.1, was selected as the recipient strain. A similar transformation procedure was carried out as shown in Fig. 5A using the same *cnaA*-sgRNA1 and *hph* with MHAs as the repair template. As a result, 97% colonies selected randomly had a phenotype similar to that of *ΔcnaA*, too (Fig. 5C). Furthermore, the results indicated that all six independent colonies among the tested transformants had an expected cleavage site with an insertion of the *hph* selectable marker. Thus, all data suggest that the MMEJ-CRISPR system supported by *in vitro* transcribed sgRNA could efficiently and precisely induce mutagenesis in *cnaA* in a Ku-independent manner.

3.6. Precise and efficient in-frame integration of an exogenous GFP tag at the predicted site without marker insertion

Protein fusion tags are indispensable tools for purifying protein, detecting the localization of protein, determining the expression level of a gene and charactering protein–protein interactions. Tagging a protein at the N- or C-terminus mainly depends on the tertiary protein structures, protein types and distributions of domains. The strategy to tag a protein at the C-terminus involves inserting a cassette consisting of a tag and a marker in front of the stop codon (Cai et al., 2015). Inserting a tag between the ATG

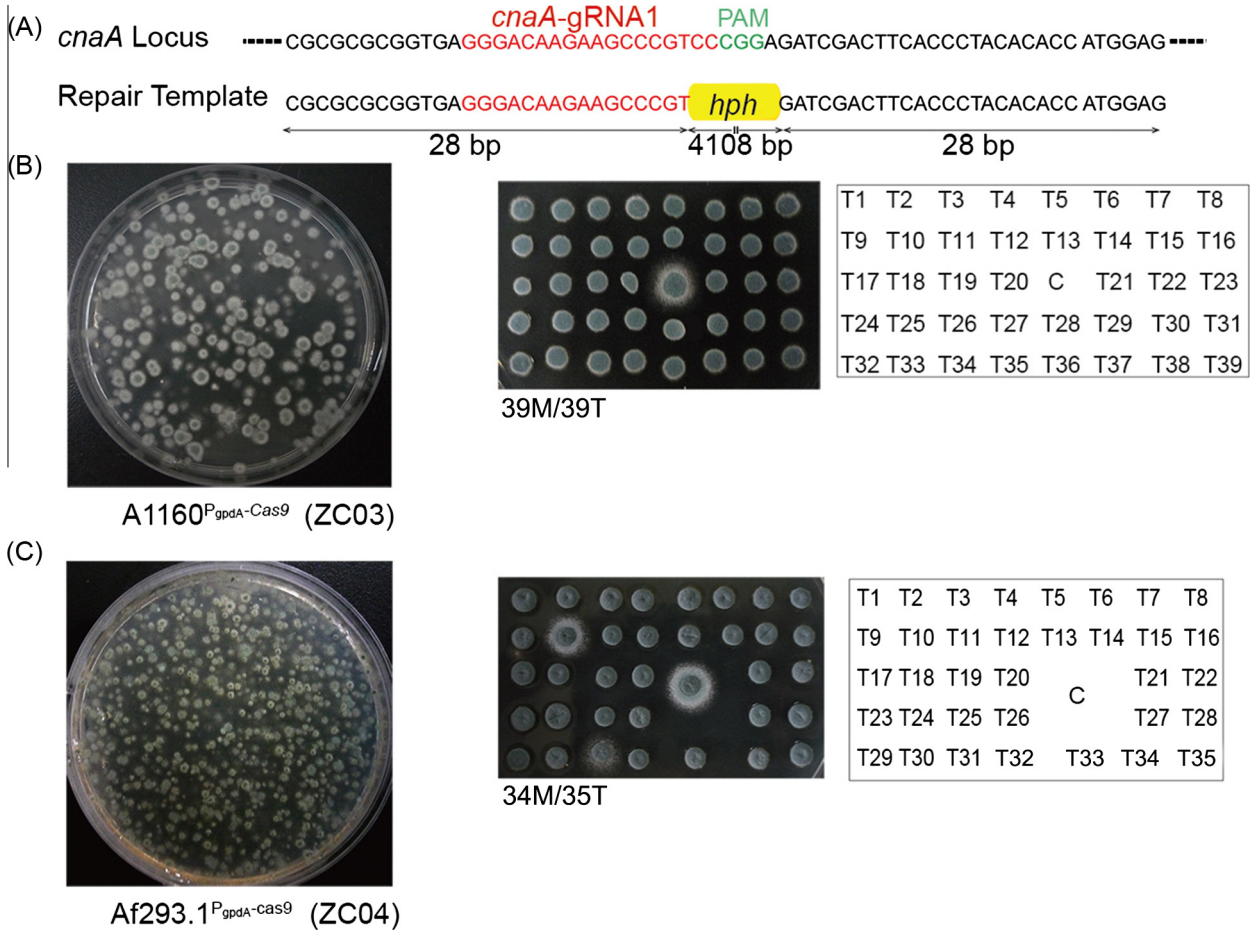

Fig. 5. Highly efficient CRISPR mutagenesis by MMEJ is Ku-independent. (A) Schematic illustration for designing the 18-nt truncated cnaA-gRNA1 sequence (red) and PAM (green) at the *cnaA* locus. (Bottom) Schematic illustration for designing the repair template *hph* flanked by two 28-bp MHAs located proximally to the PAM site. (B) (Left) Numerous transformants appeared on the transformation plate of *cnaA* mutagenesis. The ZC03 was used as the recipient strain. (Middle) Plate assays (The 2 μL sterile aqueous suspension containing the moderate spores of transformants was spotted onto YAG medium). The 39M/39T indicated that there were 39 mutant strains among the 39 transformants selected at random. The C indicated control (ZC03) and the T indicated transformants. (C) The results were similar to the previously described in (B) when wild-type *ku80* Af293.1$^{PgpdA\text{-}Cas9}$ (ZC04) strain was used as recipient strain. (For interpretation of the references to color in this figure legend, the reader is referred to the web version of this article.)

start codon and promoter is a more complex process, which also relies on marker insertion into the target gene. To date, a common strategy to introduce a GFP tag into the N-terminus of a target protein was reported in *A. nidulans* using five-piece fusion PCR (Wong et al., 2008). However, they are complicated by multiple high-fidelity fusions PCR. With the aim of solving this problem, we tried to set up an *in situ* tag-insertion method by using the above-described MMEJ-CRISPR system (Fig. 6A). We designed a gRNA (*cnaA*-gRNA2) targeting the start codon and generated GFP fragments harboring 39-bp MHAs located proximally to the PAM site. Since the right MHA of GFP repair template includes a copy of *cnaA*-gRNA2-PAM, to get rid of the possibility that this right MHA could be edited by Cas9 after GFP integration, we introduced a silent mutation at the PAM site to avoid to be recognized by Cas9 but this mutation could not affect function for CnaA (Fig. 6B). To create an in-situ GFP tag fused to N-terminus of CnaA without any selection marker insertion at *cnaA* locus, we co-transformed the *cnaA*-sgRNA2 (*in vitro* transcription), GFP repair template and *hph* fragment as a selective marker, which may insert into genome randomly. Consistent with the above indels mutagenesis efficiency, diagnostic PCR analysis confirmed that all isolated colonies (we have checked six independent clones) had GFP integration at the predicted site of *cnaA* (Fig. S2B). Furthermore, GFP-CnaA localization patterns during germination and hyphal growth were investigated by fluorescent microscopy. Consistent with the previous finding, GFP-CnaA was mainly localized on septa and hyphal tips (Fig. 6C) (Juvvadi et al., 2008, 2011). These data indicate that the MMEJ-CRISPR system can precisely and efficiently manipulate in-frame integration of an exogenous GFP tag at the predicted site without marker insertion.

3.7. Simultaneous mutagenesis of multiple genes by the MMEJ-CRISPR system

To further test whether the MMEJ-CRISPR system could facilitate multi-locus genomic mutagenesis in *A. fumigatus*, we simultaneously introduced two edits into *pksP* and *cnaA* with one selection marker *hph*. For the mutagenesis of *pksP*, we designed a new sgRNA (*pksP*-sgRNA2) directing against exon 3 of *pksP* and generated a repair template including two premature stop codons as substitutes in the PAM area. For *cnaA* mutagenesis, we employed the same aforementioned *cnaA*-sgRNA1 and the relative repair template (Fig. 7A). Then, we co-transformed two sgRNAs with related repair template as mentioned above into ZC03 under hygromycin selection. As a result, all albino colonies tested displayed a compacted colony phenotype with a strikingly deficient polar growth similar to that of *ΔcnaA* colonies (Fig. 7B). Six suspected double mutants were streak purified, and after identification by diagnostic PCR and sequencing, 100% of tested transformants showed the two predicted changes in *pksP* and *cnaA* (Fig. S2C). Together, these results suggest that the *Aspergillus* MMEJ-CRISPR system permits the simultaneous and highly efficient mutagenesis of multiple genes.

4. Discussion

Currently, approaches for uncovering the functions of previously uncharacterized genes in filamentous fungi are based on the identification of loss-of-function phenotypes that occur following the homologous recombination-mediated knock-out or

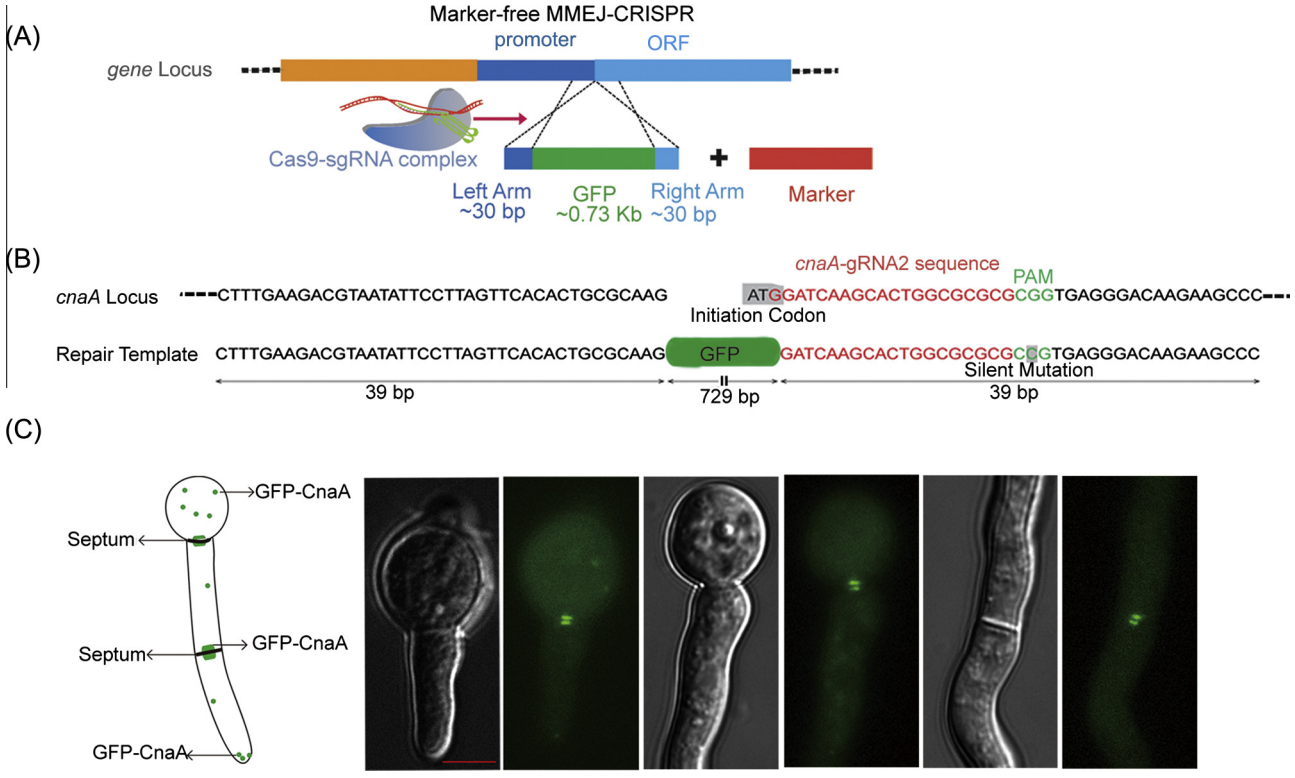

Fig. 6. Precise and efficient in-frame integration of an exogenous GFP tag at the predicted site without marker insertion. (A) Schematic illustration of inserting a GFP tag at N-terminus using the MMEJ-CRISPR system. The system contains a Cas9-sgRNA complex targeting the start codon region, the free marker gene and a GFP fragment harboring MHAs located proximally to the PAM site. (B) Schematic illustration of the guide sequence (*cnaA*-gRNA2) at the *cnaA* locus and the GFP repair template with MHAs that contains a silent mutation at the PAM site. (C) The GFP-CnaA localization after growth for 12 h at 37 °C was observed at the septa, hyphal tips and cytoplasm. The bar length is 5 μm.

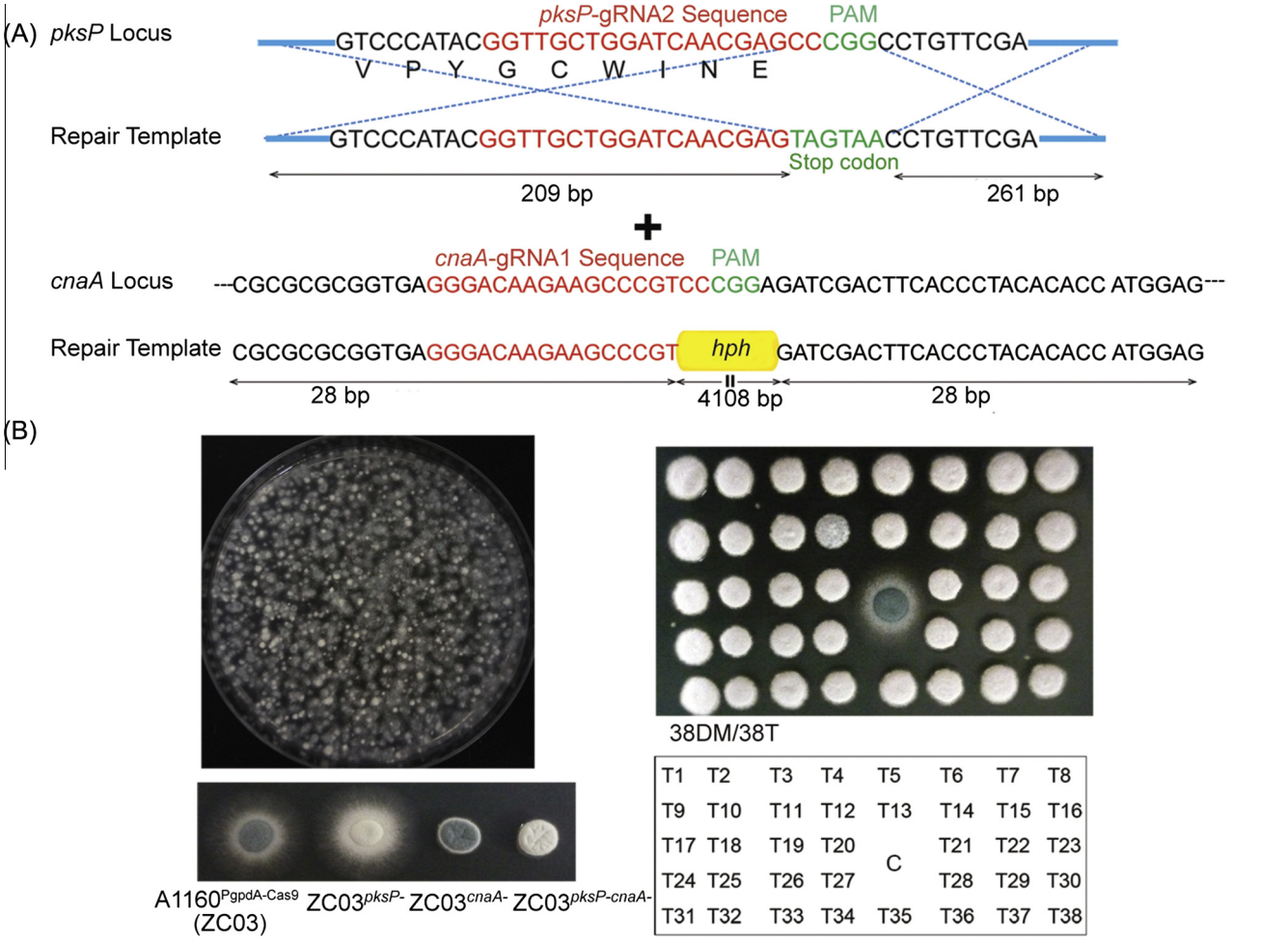

Fig. 7. Simultaneous mutagenesis of multiple genes by the MMEJ-CRISPR system. (A) Schematic illustration of the two gRNA sequences and two repair templates for *pksP* and *cnaA* mutagenesis. (B) (Left) The relative transformation plate for simultaneous mutagenesis of *pksP* and *cnaA*. Phenotypic comparison of ZC03^{pksP-} (ZC06), ZC03^{cnaA-} (ZC07), ZC03$^{pksP\text{-}cnaA-}$ (ZC10) and their parental strain ZC03 on YAG medium. (Right) The albino colonies were derived from the transformation plate for double mutation. The label 38DM/38T indicated that there were 38 predicted double mutants among randomly selected 38 transformants.

knock-in of a gene (Schoberle et al., 2013; Szewczyk et al., 2006). Although gene targeting is possible in *A. fumigatus*, homologous recombination during transformation is not particularly efficient. Because filamentous fungi have a dominant NHEJ DNA repair pathway that competes with homology-directed repair (HDR), the majority of transforming sequences integrate heterologously. To improve homologous integration efficacy, deletion of *ku80*, a homolog of the human *ku70* gene required for non-homologous end joining, combined with heterologous selectable markers are required to obtain useful frequencies of homologous integration. In addition, although gene targeting was efficient with 500-bp flanking regions, fewer transformants were obtained than with 1000- and 2000-bp flanking regions (da Silva Ferreira et al., 2006; Krappmann et al., 2006b). Thus, the labor used to construct targeting vectors and difficulties in inducing HDR in wild-type or clinical isolates of *A. fumigatus* represent technical hurdles for the application of HDR-mediated knock-in or knock-out technology. Nevertheless, it is impossible to carry out multiple gene mutageneses by sexual crossing for the majority of *A. fumigatus* isolates of unknown mating type (O'Gorman et al., 2009; Sugui et al., 2011). Clinical isolates that have a wild-type *ku80* background without any nutritional selection marker especially suffer from low homologous integration efficacy or the use of complex marker-dependent chromosomal integration strategies. In addition, traditional homologous integration technology has its limitations and is incompatible with *in situ* mutagenesis screens on a genome-wide scale.

CRISPR-Cas9-based editing has drawn the attentions of biology workers of the whole word due to the unprecedented control over animal, plant, microbe, and many other organism genomes. Thus, the advent of the CRISPR/Cas9 system of gene disruption has ushered in a new era of genetic investigation. As we know, forward genetic screens are powerful tools for the discovery and functional annotations of genetic elements with genome-scale guide RNA libraries for unbiased, phenotypic screening including knock-out approaches that inactivate genomic loci and strategies that modulate transcriptional activity. Compared to its use in mammalian systems, application of the CRISPR-Cas9 system in filamentous fungi is still in a preliminary state, there are a few recent reports regarding the use of the CRISPR-Cas9 system to perform loss-of-function studies in several *Aspergillus* species. In *A. fumigatus* in particular, the CRISPR-Cas9 system can indeed be used to target the *A. fumigatus* polyketide synthase gene (*pksP*) via the NHEJ pathway, and the constitutive expression of the Cas9 nuclease by itself is not deleterious with respect to *A. fumigatus* growth or virulence (Fuller et al., 2015). Compared to the recently established CRISPR/Cas9 system for targeted gene disruption in *A. fumigatus* that has an efficiency of 25–53% and occurs through a mechanism independent of the homologous repair machinery, we are able to efficiently

and simultaneously target one or multiple genomic sites and introduce changes via very short (approximately 35-bp) homology arms in a process referred to as microhomology-mediated end joining (MMEJ). We employed the CRISPR-Cas9 genome-editing tool for an exploratory analysis of targeted genes *via* MMEJ with a fragment flanked by approximately 35-bp homology arms. Our CRISPR-Cas9 system is capable of introducing targeted double-strand breaks (DSBs) into DNA and enables precise genome editing by increasing the rate at which externally supplied DNA fragments. Most importantly, through this new approach, we can carry out precise and efficient in-frame integration of an exogenous GFP tag at the predicted site without marker insertion (approximately 95–100% accuracy rate). Protein fusion tags are indispensable tools for verifying protein characterization. Tagging a protein at the N- or C-terminus mainly depends on the tertiary protein structure, protein type and distribution of the domains. Employing a common strategy using five-piece fusion PCR, inserting a tag between the ATG start codon and promoter, is a complex process, which also relies on marker insertion at the target gene. We designed a sgRNA (*cnaA*-sgRNA2) against the start codon region and generated GFP fragments flanked by 39-bp homology arms located proximally to the PAM site. Notably, to get rid of the possibility that this short microhomology arm could be edited again by Cas9 after integration, we introduced a silent mutation based on the codon degeneracy and wobble at the PAM site to avoid to be recognized by Cas9 but this mutation could not affect function for this target gene (Kim et al., 2014).

Our data indicate that with constitutive expression of Cas9, the MMEJ-CRISPR system can be manipulated precisely and efficiently in-frame integration of an exogenous GFP tag at the predicted site without marker insertion. Moreover, the MMEJ-CRISPR system permits the simultaneous and highly efficient mutagenesis of multiple genes with or without marker insertion. Notably, we successfully truncated the conidial melanin gene *pksP* without marker insertion at the *pksP* locus. Thus, the MMEJ-mediated CRISPR-Cas9 method enables rapid and efficient genome manipulation and unlocks the CRISPR toolset for use in *A. fumigatus*. This system provides new opportunities for uncovering the functions of previously uncharacterized virulence and susceptibility genes in antifungals and for screening/identifying the specific peptide regions in the target protein so that blocking this region can kill or inhibit pathogen viability while inducing fewer side effects in the host. Most importantly, the development and successful application of the MMEJ-CRISPR system for genome engineering should have broad applications to other medicinal and industrial filamentous fungi because they all have conserved homology-directed repair pathways.

Acknowledgments

This work was financially supported by the National Natural Science Foundation of China (NSFC81330035 and NSFC31370112) to L. Lu; the Special Fund for the Doctoral Program of Higher Education of China (No. 20123207110012) to L. Lu; the Priority Academic Program Development (PAPD) of Jiangsu Higher Education Institutions. *A. fumigatus* strain A1160, Af293 and Af293.1 were obtained from FGSC (http://www.fgsc.net). We thank Guangshuo Ou and Zhongfu Shen (Tsinghua-Peking Center for Life Sciences) for kindly providing pX330 and helpful comments on the manuscript. We thank Meng Feng for providing language help.

Appendix A. Supplementary material

Supplementary data associated with this article can be found, in the online version, at http://dx.doi.org/10.1016/j.fgb.2015.12.007.

References

Aleksenko, A., Clutterbuck, A.J., 1997. Autonomous plasmid replication in *Aspergillus nidulans*: AMA1 and MATE elements. Fungal Genet. Biol. 21, 373–387.
Cai, Z.D. et al., 2015. The Gbeta-like protein CpcB is required for hyphal growth, conidiophore morphology and pathogenicity in *Aspergillus fumigatus*. Fungal Genet. Biol. 81, 120–131.
da Silva Ferreira, M.E. et al., 2007. Functional characterization of the *Aspergillus fumigatus* calcineurin. Fungal Genet. Biol. 44, 219–230.
da Silva Ferreira, M.E. et al., 2006. The *akuB*^{KU80} mutant deficient for nonhomologous end joining is a powerful tool for analyzing pathogenicity in *Aspergillus fumigatus*. Eukaryot. Cell 5, 207–211.
Denning, D.W., Bromley, M.J., 2015. How to bolster the antifungal pipeline. Science 347, 1414–1416.
Denning, D.W. et al., 2011. Global burden of chronic pulmonary aspergillosis as a sequel to pulmonary tuberculosis. Bullet. World Health Organ. 89, 864–872.
Denning, D.W. et al., 2013. Global burden of allergic bronchopulmonary aspergillosis with asthma and its complication chronic pulmonary aspergillosis in adults. Med. Mycol. 51, 361–370.
DiCarlo, J.E. et al., 2013. Genome engineering in Saccharomyces cerevisiae using CRISPR-Cas systems. Nucleic Acids Res. 41, 4336–4343.
Doudna, J.A., Charpentier, E., 2014. Genome editing. The new frontier of genome engineering with CRISPR-Cas9. Science 346, 1258096.
Dyer, P.S., O'Gorman, C.M., 2012. Sexual development and cryptic sexuality in fungi: insights from *Aspergillus* species. FEMS Microbiol. Rev. 36, 165–192.
Farboud, B., Meyer, B.J., 2015. Dramatic enhancement of genome editing by CRISPR/Cas9 through improved guide RNA design. Genetics 199, 959–971.
Fox, D.S., Heitman, J., 2002. Good fungi gone bad: the corruption of calcineurin. Bioessays 24, 894–903.
Fu, Y. et al., 2014. Improving CRISPR-Cas nuclease specificity using truncated guide RNAs. Nat. Biotechnol. 32, 279–284.
Fuller, K.K. et al., 2015. Development of the CRISPR/Cas9 system for targeted gene disruption in *Aspergillus fumigatus*. Eukaryot. Cell. http://dx.doi.org/10.1128/EC.00107-15.
Gravelat, F.N. et al., 2012. Targeted gene deletion in *Aspergillus fumigatus* using the hygromycin-resistance split-marker approach. Methods Mol. Biol. 845, 119–130.
Hill, J.A. et al., 2013. Genetic and genomic architecture of the evolution of resistance to antifungal drug combinations. PLoS Genet. 9, e1003390.
Hsu, P.D. et al., 2013. DNA targeting specificity of RNA-guided Cas9 nucleases. Nat. Biotechnol. 31, 827–832.
Hu, W. et al., 2007. Essential gene identification and drug target prioritization in *Aspergillus fumigatus*. PLoS Pathog. 3, e24.
Jacobs, J.Z. et al., 2014. Implementation of the CRISPR-Cas9 system in fission yeast. Nat. Commun. 5, 5344.
Jiang, H. et al., 2014. Deletion of the putative stretch-activated ion channel Mid1 is hypervirulent in *Aspergillus fumigatus*. Fungal Genet. Biol. 62, 62–70.
Jinek, M. et al., 2012. A programmable dual-RNA-guided DNA endonuclease in adaptive bacterial immunity. Science 337, 816–821.
Juvvadi, P.R. et al., 2008. Calcineurin localizes to the hyphal septum in *Aspergillus fumigatus*: implications for septum formation and conidiophore development. Eukaryot. Cell 7, 1606–1610.
Juvvadi, P.R. et al., 2011. Localization and activity of the calcineurin catalytic and regulatory subunit complex at the septum is essential for hyphal elongation and proper septation in *Aspergillus fumigatus*. Mol. Microbiol. 82, 1235–1259.
Kim, H. et al., 2014. A Co-CRISPR Strategy for efficient genome editing in *Caenorhabditis elegans*. Genetics 197, 1069–1080.
Krappmann, S. et al., 2006a. Gene targeting in *Aspergillus fumigatus* by homologous recombination is facilitated in a nonhomologous end-joining-deficient genetic background. Eukaryot. Cell 5, 212–215.
Krappmann, S. et al., 2006b. Gene targeting in *Aspergillus fumigatus* by homologous recombination is facilitated in a nonhomologous end-joining-deficient genetic background. Eukaryot. Cell 5, 212–215.
Langfelder, K. et al., 1998. Identification of a polyketide synthase gene (*pksP*) of *Aspergillus fumigatus* involved in conidial pigment biosynthesis and virulence. Med. Microbiol. Immunol. 187, 79–89.
Liu, F.F. et al., 2015a. Calcium signaling mediates antifungal activity of triazole drugs in the *Aspergilli*. Fungal Genet. Biol. 81, 182–190.
Liu, R. et al., 2015b. Efficient genome editing in filamentous fungus *Trichoderma reesei* using the CRISPR/Cas9 system. Cell Discov. 1, 15007.
Nielsen, M.L. et al., 2006. Efficient PCR-based gene targeting with a recyclable marker for *Aspergillus nidulans*. Fungal Genet. Biol. 43, 54–64.
Nodvig, C.S. et al., 2015. A CRISPR-Cas9 system for genetic engineering of filamentous fungi. PLoS One 10, e0133085.
O'Gorman, C.M. et al., 2009. Discovery of a sexual cycle in the opportunistic fungal pathogen *Aspergillus fumigatus*. Nature 457, 471–474.
Ran, F.A. et al., 2013. Genome engineering using the CRISPR-Cas9 system. Nat. Protoc. 8, 2281–2308.
Ryan, O.W. et al., 2014. Selection of chromosomal DNA libraries using a multiplex CRISPR system. Elife 3.
Schoberle, T.J. et al., 2013. Plasmids for increased efficiency of vector construction and genetic engineering in filamentous fungi. Fungal Genet. Biol. 58–59, 1–9.
Shalem, O. et al., 2015. High-throughput functional genomics using CRISPR-Cas9. Nat. Rev. Genet. 16, 299–311.
Steinbach, W.J. et al., 2006. Calcineurin controls growth, morphology, and pathogenicity in *Aspergillus fumigatus*. Eukaryot. Cell 5, 1091–1103.

Sugui, J.A. et al., 2011. Identification and characterization of an *Aspergillus fumigatus* "supermater" pair. MBio 2.
Szewczyk, E. et al., 2006. Fusion PCR and gene targeting in *Aspergillus nidulans*. Nat. Protoc. 1, 3111–3120.
Tsai, H.F. et al., 1998. The developmentally regulated alb1 gene of *Aspergillus fumigatus*: its role in modulation of conidial morphology and virulence. J. Bacteriol. 180, 3031–3038.
Vyas, V.K. et al., 2015. A *Candida albicans* CRISPR system permits genetic engineering of essential genes and gene families. Sci. Adv. 1, e1500248.
Wei, X. et al., 2015. The molecular mechanism of azole resistance in *Aspergillus fumigatus*: from bedside to bench and back. J. Microbiol. 53, 91–99.
Wong, K.H. et al., 2008. Sumoylation in *Aspergillus nidulans*: sumO inactivation, overexpression and live-cell imaging. Fungal Genet. Biol. 45, 728–737.
Xue, T. et al., 2004. Isogenic auxotrophic mutant strains in the *Aspergillus fumigatus* genome reference strain Af293. Arch. Microbiol. 182, 346–353.